

In particular, we require that this determinant be finite and nonzero for some range of $\boldsymbol{\xi}$ values at any \mathbf{y} where the high frequency inversion is to be computed.

The expression of the spatial weighting in terms of this one determinant for any source-receiver configuration and background propagation speed is a major contribution of Beylkin's [Beylkin, 1985] approach to high-frequency inversion. For this reason, we refer to this determinant as the *Beylkin determinant*.

Much more extensive discussion of this inversion procedure can be found in Bleistein et al. [1998].

Implementations of this result for a hierarchy of more difficult background velocities and source/receiver configurations have been carried out. See Sumner [1988a, b], Xu [1996a, b]. More are in development.

Determination of $\cos \theta_s$.

When the operator in (26) is applied to Kirchhoff-approximate data, we find that, indeed, the output is asymptotically equal to the singular function of the reflecting surface multiplied by a "slowly varying" spatial factor as in (8). At the peak value of the singular function on the reflector—where $\phi = 0$ in (8)—the amplitude in that equation becomes

$$\beta_{\text{peak}} \sim R(\mathbf{y}, \theta_s) \frac{\cos \theta_s}{\pi c(\mathbf{y})} \int_{-\infty}^{\infty} F(\omega) d\omega, \quad \text{for } \mathbf{y} \text{ on } S. \quad (27)$$

Here, R is the geometrical optics reflection coefficient at a distinguished specular angle, θ_s ; this is the angle associated with the source/receiver pair for which the incident and reflection angles at the reflection point satisfy Snell's law.

We arrive at this result by applying the method of multi-dimensional stationary phase in the variables that parametrize the reflector and the variables that parametrize the upper surface. Furthermore, we find that at stationarity,

$$|\nabla_{\mathbf{y}} \tau(\mathbf{y}, \boldsymbol{\xi})| = \frac{2 \cos \theta_s}{c(\mathbf{y})}. \quad (28)$$

More precisely, half the opening angle between the specular rays at stationarity agrees with the specular incidence angle. This suggests that we introduce a second inversion operator, $\beta_1(\mathbf{y})$,

$$\beta_1(\mathbf{y}) = \frac{1}{8\pi^3} \int d^2 \xi \frac{|h(\mathbf{y}, \boldsymbol{\xi})|}{a(\mathbf{y}, \boldsymbol{\xi}) |\nabla_{\mathbf{y}} \tau(\mathbf{y}, \boldsymbol{\xi})|^2} \int i\omega d\omega e^{-i\omega \tau(\mathbf{y}, \boldsymbol{\xi})} u_S(\mathbf{x}_g, \mathbf{x}_s, \omega). \quad (29)$$

Note the only difference between this operator and β in (26) is the power of $|\nabla_{\mathbf{y}} \tau|$ in the denominator. However, we see from (28) that this is exactly the power we need so that the peak value of this output will be

$$\beta_{1\text{peak}}(\mathbf{y}) \sim R(\mathbf{y}, \theta_s) \frac{1}{2\pi} \int F(\omega) d\omega, \quad \text{for } \mathbf{y} \text{ on } S. \quad (30)$$

Now, the ratio of peak outputs can be used to estimate the cosine of the specular angle. Then, either of the peak values provides an estimate of the reflection coefficient at that specular angle.

A typical seismic survey provides data for many common shot inversions or many common offset inversions. For each of them, the specular angle at a particular output point will be different, as will the corresponding reflection coefficient. Thus, it is possible to generate a table of estimates of reflection coefficient as a function of offset angle. Then, a nonlinear optimization technique could be used to unravel the reflection coefficient in order to estimate the change in medium parameters across the reflector. Such an estimate provides a means of determining a “best guess” in the presence of noise in real data.

On the other hand, our experience with synthetic data is that the estimate of $\cos \theta_s$ is usually about an order of magnitude better than the estimate of the reflection coefficient. We believe that this is true because the two operators are quite similar and are likely to have the same numerical artifacts and to respond the same way to noise in the data. We expect the quotient of these two operators then to “cancel” these effects to a degree, leading to the higher accuracy of the output.

We remark that the same method can be used to find other geometrical attributes of the data. One need only introduce new operators that differ from β or β_1 by the appropriate geometrical optics factor in the background model parameters. Thus, one could estimate the specular traveltimes from source and receiver, the location of the source and receiver, the normal to the reflector (which is in the same direction as $\nabla_y \tau$ at stationarity) and other attributes, as well. See Geoltrain and Chovet [1991].

We remark that these estimates of reflection coefficient and specular angle depend strongly on the assumption that there are no caustics in the specular ray field to the reflection process and, further, that there is no multi-pathing. The former problem can be overcome if the separate “legs” of the multiple arrivals are processed separately. The latter problem requires that we change the structure of the Green’s function for those ray trajectories that have passed through a caustic. Work on this is currently in progress. See de Hoop’s article in this volume, and de Hoop [1998].

Two-and-one-half Dimensions.

Though computer technology has advanced to permit the processing of areal surveys as single data sets, line-by-line processing of seismic data is still widely used because of the obvious cost benefits. Equation (26) cannot be used to process a single line of data. In fact, a single line of data cannot be used to reconstruct a 3D medium.

There are situations, however, where the gathering and/or processing of a single line of data will suffice to produce an adequate inversion for the interior medium. Suppose, for example that in a given region, the parameter variations were (nearly) two dimensional such that the primary variations in the subsurface parameters were

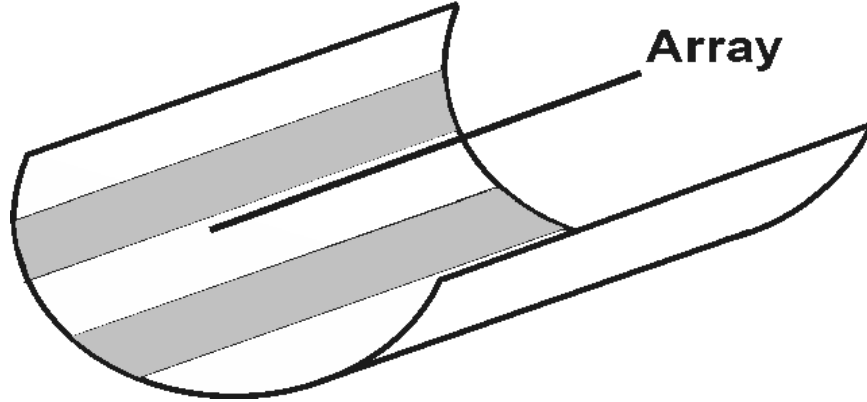


FIG. 4. The black line depicts a source-receiver array located on the axis of a buried half-cylinder. The strips of grey are only two of the many possible zones on the half-cylinder that could be represented by the data collected by the array.

in one transverse direction.

Let us designate that direction as the direction of maximal dip and the orthogonal direction as the direction of strike. It is reasonable to expect that data gathered along the maximum dip direction of such a model will provide enough information to invert for the profile.

Mathematically, we idealize the problem as follows. Assume that the medium parameters vary only in one transverse direction, say x and in depth, z . Let the survey be conducted along a line in the x -direction, at a particular y value, say at $y = 0$. Our first objective, therefore, is to invert this one line of data to produce an image of the subsurface. See Figure 5.

The reader should realize that this is *not* a two-dimensional inversion problem. The medium is still three dimensional; our sources are point sources in three dimensions with all their three dimensional propagation characteristics. The 3D acoustic wave equation is still the governing equation for the problem. Only the nature of the medium parameters and our fortuitous choice of experimental line suggest a two dimensional problem. A fully two dimensional problem would be equivalent to using *line sources* in this three dimensional world, with quite different propagation characteristics. (In 2D, the incident wave has nonzero energy propagating through the plane, $y = 0$, for *all time* greater than zero, and all spatial positions. This is in contrast to the 3D incident wave, which passes through a given range from the source at a given time and is gone after a time governed only by the duration of the source.)

We will refer problems involving three dimensional wave propagation in media having only two dimensional parameter variability as *two-and-one-half dimensional* (2.5D) problems. The key to solving the 2.5D inverse problem is to realize that there really is enough information from a single line of data to solve the three dimensional inverse problem, as long as the medium parameters really depend on only two vari-

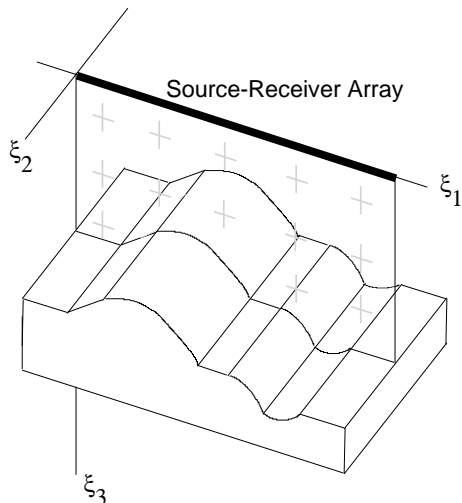


FIG. 5. The black line depicts a source-receiver array located over a 2.5-D model. All specularly reflecting raypaths are confined to the plane, $\xi_2 = 0$.

ables.

Given such a line of data, say at $\xi_2 = x_{s2} = x_{g2} = 0$, we propose the following

Thought experiment: Consider the data for which the entire source-receiver array for each experiment in the ensemble of experiments is moved to any line, ξ_2 , different from zero, and

Claim: The data for the ensemble of experiments on the new line are exactly the same as the data for the ensemble of experiments on the line at $\xi_2 = 0$.

In this case, note that the data in (26) is independent of the out-of-plane variables and only the operator kernel depends on ξ_2 . It is possible, then, to carry out the integration in the ξ_2 direction by the method of stationary phase. The details of that discussion can be found in Bleistein, et al. [1998] and we only report on those results, here.

The condition of stationarity requires that $\xi_2 = y_2$. Evaluation of the integrand at stationarity leads to an operator that is independent of y_2 with all quantities of the integrand determinable and identical in any vertical plane, $y_2 = \text{constant}$. That is, we only need the in-plane rays, a two-dimensional in-plane Jacobian to account for amplitude variations and a two-dimensional Beylkin determinant. The out-of-plane effects are accounted for by phase shifts and “out-of-plane geometrical spreading effects” that are completely characterized in terms of a ray parameter that we call σ . This parameter is related to the 2D arclength s along a ray by

$$\frac{ds}{d\sigma} = |\nabla\tau| = \frac{1}{c(\mathbf{x})}. \quad (31)$$

After carrying out the stationary phase calculation alluded to, above, we derive the following formula for 2.5D inversion for reflectivity.

$$\beta(\mathbf{y}) = \frac{1}{[2\pi]^{5/2}} \int d\xi \frac{|H(\mathbf{y}, \xi)|}{a(\mathbf{y}, \xi)|\nabla_{\mathbf{y}}\tau(\mathbf{y}, \xi)|} \frac{\sqrt{\sigma_s + \sigma_g}}{\sqrt{\sigma_s\sigma_g}} \cdot \int \sqrt{|\omega|} d\omega e^{-i\omega\tau(\mathbf{y}, \xi) + i\pi/4 \operatorname{sgn} \omega} u_S(\mathbf{x}_g, \mathbf{x}_s, \omega). \quad (32)$$

Here, all vectors are two dimensional. Keeping with our formalism of eliminating y_2 through stationary phase, $\mathbf{y} = (y_1, y_3)$. Furthermore, ξ is now a scalar variable labeling the positions of the source and receiver on the acquisition surface. In addition, σ_s and σ_g are just the parameters σ defined in (31), above, but evaluated along the rays from \mathbf{x}_s and \mathbf{x}_g to the output point, \mathbf{y} .

The processing now has a 2D Beylkin determinant, H , given by

$$H(\mathbf{y}, \xi) = \det \begin{bmatrix} \nabla_{\mathbf{y}}\tau(\mathbf{y}, \xi) \\ \frac{\partial}{\partial \xi} \nabla_{\mathbf{y}}\tau(\mathbf{y}, \xi) \end{bmatrix}. \quad (33)$$

Implementations of this result for a hierarchy of more difficult background velocities and source/receiver configurations have been carried out. See Docherty [1987, 1998, 1991], Emanuel [1989], Geoltrain [1989], Hsu [1192], Liu [1993], Sumner [1990], Ou [1995].

KIRCHHOFF DATA MAPPING

“Kirchhoff data mapping” (KDM) is a process for transforming data from one prescribed source/receiver configuration and model of the propagating medium to another configuration and model. KDM is a “true amplitude” process in the following sense.

1. Travel time and point source geometrical spreading effects of the input configuration are transformed to those effects of the output configuration.
2. Reflector curvature geometrical spreading effects of the input configuration are transformed to those effects of the output configuration.

However, the reflection coefficient of the input configuration is preserved in the output data. On the other hand, the formalism provides a mechanism for determining both the input and the output geometrical optics incidence angles of the reflection process in these applications, thereby providing a basis for amplitude-versus-angle (AVA) analysis. Both of these transformations are model consistent; that is, they depend on the input and output physical models that are assumed for the processing.

This research is grounded in the process of *transformation to zero offset* (TZO)—the true amplitude mapping of data from finite offset between source and receiver to zero offset. The constant background specialization of that technique is the *Normal MoveOut/Dip MoveOut* [NMO/DMO] method, which are standard tools in seismic data processing [Artley and Hale, 1994, Black, et al, 1993, Gardner and Forel, 1988, 1995, Hale, 1984, Hale and Artley, 1993, Liner, 1990, 1991]. The research was initially motivated by a desire to develop a specific technology and computer software for TZO in a depth-dependent earth model. That application is reported on separately in Jaramillo [1998, Jaramillo and Bleistein, 1998a, 1998b]. It extends the earlier NMO/DMO process in depth dependent background of Artley and Hale [1992] and Hale and Artley [1993] to a true amplitude process.

The basic idea of these methods is to cascade an inversion formula with a modeling formula. The combined formula maps a given data set to another. Both of the operators used are integral operators. Thus, the result is an integral over the variables of the input data set—here denoted by ξ_I and ω_I —to produce an estimated model of a reflectivity in the subsurface combined with an integral over the coordinates of that model—here denoted by \mathbf{x} —to produce the output data set—with variables ξ_O and ω_O .³ The input data set depends only on the variables of the acquisition geometry and time (or frequency)—the variables ξ_I and ω_I . The operator is a function of the input and output parameters and the reflectivity model variables, as well; that is, all of the variables introduced above. The idea, then, is to carry out the integration over (earth modeling) variables, \mathbf{x} , asymptotically, to obtain a weight that is a function of the input and output variables, only. This weight is then applied to the input data set to produce the output data set. It is this asymptotic analysis that can only be partially carried out in the absence of an explicit KDM implementation; hence, the word, “platform,” to characterize this point of departure from which to derive the mapping of specific implementations.

KDM options.

Below, is a list some possible mappings of data sets from an input macro-model and source/receiver configuration to an alternative data set on output. All of these can be carried out in 2D, 2.5D and 3D.

1. **Offset continuation and TZO.** KDM is not limited to transforming to zero-offset; the formula lends itself to analysis of the transformation of data from one offset to another, with TZO as a special case. That is, (36) and (37), below, provide a platform for *offset continuation* along the lines of Fomel [1995a,b, 1996, 1997] and Fomel et al [1996]. However, as soon as one applies to the platform equations the type of asymptotic analysis that leads to the classical

³In this notation, the source and receiver coordinates are given parametrically as functions of the variables ξ_I and ξ_O , respectively. By this device, specification of the source/receiver configurations is postponed to specific applications.

NMO/DMO-type data mapping, the mapping requires “large” (e.g., a few wave lengths) change in offset to be valid.

2. **Transformation of common-offset data to common-shot data.** In this case, the transformed data represents the response from a single shot at an array of receivers covering the upper surface. Such data has the advantage that it is the solution of the wave equation, whereas common-offset (and zero-offset) data are a collection of single responses to an ensemble of wave equations, one for each shot. This ensemble data is not a solution of the wave equation, although it is treated as such in *wave equation migration*.
3. **Mapping of data from variable background propagation parameters to constant background parameters.** Time sections in constant background media are easier to interpret. It is not clear to us at this point, however, how multi-paths will map, nor how data from vertical and overhung reflectors will map. We expect singularities of the mapping process for these cases. On the other hand, where the method works, it opens the mapped data set to a much broader suite of applicable migration/inversion programs and related analysis techniques.
4. **“Unconverting” mode-converted waves.** For example, one could map the scalar components of P-SV data to the scalar components of P-P data [Chan and Stewart, 1996]. If the “true” P-P data were available, a comparison of this latter data set with the mapped data set could provide a check on the assumptions made in the macro-model for the converted wave propagation. Furthermore, again, there are many more processing options available for P-P data than for mode converted data. This mapping would provide a means of extending the range of processing options once the data is mapped.
5. **Velocity analysis.** When data from a suite of offsets are all mapped to zero offset, events should line up. To the extent that they do not, they provide the same type of information about velocity errors as does a common trace gather of a suite of prestack migrations/inversions.
6. **Wave equation datuming.** The acquisition surface can be changed for both the sources and receivers. Downward continuation of sources and receivers or mapping from irregular acquisition topography to a planar topography, are two potential datuming applications for this platform. See Sheaffer and Bleistein [1998]. For small increments in depth, the implementation of KDM provides an alternative to phase shift migration [Gazdag and Squazzero, 1984], while for larger increments in depth, the implementation of KDM provides an alternative to wave equation datuming [Berryhill, 1979].
7. **Mapping of swath data to a single line at zero azimuth.** Swath shooting is a process whereby multiple lines of receivers are used with a single shot, as

might occur if a boat towed more than one sonophone line. The data from the separate lines could be mapped to a single line that could be “straightened” to be along the line of the survey—given sufficient information about the deviation of the swath survey from that line and about the path of the boat [Biondi and Chemingui, 1994].

8. **Combinations of the above.** For example, consider the application of downward continuation of receivers (or sources). The continuation process always yields output data over a shorter line than that of the input data. Starting from a prescribed shot gather with a given cable length of receivers, the cable length of asymptotically accurate mapped data decreases from the input cable length with increasing depth. On the other hand, consider first creating a single common shot data set from the full array of common offset gathers. This new data set effectively has a “cable length” equal to the length of the survey, typically, much longer than the cable length for each shot. Now, the range of validity of the downward continuation of receivers “shrinks” from an initial length equal to the survey length. One can expect that the data can be continued much deeper into the subsurface and maintain properly transformed geometrical spreading effects and travel time corrections over a cable length that will be adequate for further processing. As a second example of cascading, consider the process of first downward continuing the receivers and then downward continuing the sources. This should provide a true amplitude simultaneous downward continuation of sources and receivers.

Derivation of a 3D Kirchhoff data mapping formula

In this section, the fundamental equation for space-frequency domain KDM in 3D will be derived. This will be done by cascading a Kirchhoff-approximate forward modeling formula with an inversion formula. Crucial to this analysis is the representation of the Kirchhoff modeling formula as a volume integral as in (15). However, in this analysis, we will want to distinguish between *input variables* and *output variables*. Thus, in that modeling formula, we will want to identify all of the variables as arising from the output background model and output source/receiver configuration. We will do so, by introducing subscripts O on all the relevant variables. Thus, the output data model is given by

$$u_O(\boldsymbol{\xi}_O, \omega_O) \sim -i\omega_O F(\omega_O) \int a_O(\mathbf{x}, \boldsymbol{\xi}_O) |\nabla_x \tau_O(\mathbf{x}, \boldsymbol{\xi}_O)| \beta(\mathbf{x}) e^{i\omega_O \tau_O(\mathbf{x}, \boldsymbol{\xi}_O)} d^3x. \quad (34)$$

Here, all of the variables are in the modeling equations of the previous section, except for the introduction of the subscript, I .

Now, the second component of the cascade process is the reflectivity function, β , determined from the input source/receiver configuration and the input earth model. Here, we use the inversion formula, (26), but now we introduce subscripts, I , to denote